Characteristics of droughts in Argentina's Core Crop Region

Leandro Carlos Sgroi [1], Miguel Angel Lovino [1,2], Ernesto Hugo Berbery [3], Gabriela Viviana Müller [1,2]

[1]Centro de Estudios de Variabilidad y Cambio Climático (CEVARCAM), Facultad de Ingeniería y Ciencias Hídricas, Universidad Nacional del Litoral, Santa Fe, Argentina

[2]Consejo Nacional de Investigaciones Científicas y Técnicas (CONICET), Santa Fe, Argentina

[3]Earth System Science Interdisciplinary Center (ESSIC)/Cooperative Institute for Satellite Earth System Studies (CISESS), University of Maryland, College Park, MD, USA

Correspondence to: Leandro C. Sgroi (lsgroi@unl.edu.ar)

Abstract. This study advances the understanding and impacts of dry episodes on wheat, corn, and soybean yields over Argentina's Core Crop Region. These major crops' production is intense and represents the country's Gross Domestic Product's main contribution. Our analysis focuses on droughts' properties, including their magnitude, frequency at different time scales, duration, and severity. We analyzed 40 years of precipitation and soil moisture anomalies and their corresponding non-parametric standardized indices at time scales of 1-, 3- and 6-months. The climate variables were complemented with 40 years of the crops' yield data. The percentage of drought occurrence in northeastern Argentina ranges between 12-18%, with the larger values located towards the Core Crop region's eastern/northeastern sector. Analysis of drought duration suggests that most cases tend to occur for periods shorter than three months, while a few can extend up to one year and even fewer longer. More importantly, regardless of the duration, droughts have larger impacts during the crops' critical growth period. Corn and soybean have their critical periods during summer and are more sensitive to precipitation and soil moisture deficits than wheat, which has its critical months during spring. Quantification of the relation between the droughts' indicators during the crops' critical periods and detrended annual crop yields was performed. Large drought severity values during the crop-sensitive months result in significant crop yield losses. Results suggest that shorter-scale indicators during sensitive periods are most appropriate to predict crop yield losses than the longer-scale indicators. This new approach can be helpful for regional decision systems that support planning by water managers and agricultural stakeholders.

1 Introduction

Southeastern South America (SESA) is a region where agriculture and cattle ranching are the primary resources and contributors to its Gross Domestic Product. In Argentina, for instance, exports of soybean, corn, and wheat and their derived products accounted for about USD 41.4 billion yearly on average for 2014-2018 (Ministry of Agriculture, Livestock, and Fisheries of Argentina, MAGyP, 2019). Most of the agriculture is rain-fed, with irrigation accounting for less than 3% of the total crop region (Siebert et al., 2013). Thus, crops and stockbreeding are susceptible to climate variability and extremes as they depend highly on natural rainfall. Corn is among the more sensitive crops to water deficits (Minetti et al., 2007), while

soybean production requires a middle range of water availability and tends to be negatively impacted by either wet or dry seasonal extremes (Penalba et al., 2007).

Droughts may have devastating economic and social impacts. Documentation of individual drought events has shown that, indeed, this is the case. The 1988/1989 drought in Argentina was ranked among the worst episodes on record. The cultivated area was reduced by about 35%, and the crop yield decreased by about 15% resulting in a 44% loss of productivity and, consequently, in high economic losses (IMF, 1990). Another severe drought episode took place during the 2003/2004 austral warm season. The drought started in September 2003 (austral spring), affecting river discharges. By April 2004, the lack of water in the Uruguay River led to the closure of 13 out of 14 turbines at the Salto Grande hydropower plant (La Nación, 2004; Penalba and Vargas, 2008). Yet another severe episode took place during 2008/2009. This drought was at the time one of the most intense, with reductions of wheat yields of about 50% and leading to the death of 1.5 million cattle heads in Argentina (Barrionuevo, 2009). The drought of late 2011/2012 had substantial impacts on soybean and corn production, causing losses of the order of USD 2.5 billion (Webber, 2012). The more recent drought between November 2017 and April 2018 caused a drop of 33% of soybean production and 15% of maize production during the 2017/2018 season with respect to the previous year (MAGyP, 2018).

Statistical analyses of extreme events in SESA have shown that periods of water deficit can occur at different time scales, with an inverse relationship between frequency and duration, i.e., shorter-lived events tend to be more frequent than those of longer duration. Hence, many observational studies of drought have centered around two approaches—first, studies based on monthly data to examine droughts' evolution at longer time scales. For instance, Minetti et al. (2007) showed that one-month-long droughts account for about 53% of all cases; two-month droughts are present in 28% of all cases, and droughts of three or more months represent less than 20% of the cases. Second, studies with daily data have shown that even relatively short dry spells can significantly impact if they occur when crops are most sensitive to water availability, as is the case during the growing season. These dry spells occur over smaller regions than those observed in monthly data, therefore with a limited damaging effect (Naumann et al., 2008). Dry spell duration is about six days on average in the Humid Pampas, although they increase in length towards the west (Penalba and Llano, 2008; Llano and Penalba, 2010; Naumann et al., 2012). Longer dry spells also present an increasing gradient from east to west, up to 60 days in the eastern sector, and about 190 days in semi-arid west (Llano and Penalba, 2010).

Dry episodes in SESA have experienced decadal and longer time changes. Changes in the frequency of dry and wet spells were reported as early as in the 19th Century by Ameghino (1884). He even proposed that such changes were due to the introduction of land-use practices in colonial times, going back to the 17th Century when water-retaining tall grass was replaced by short grass as agriculture started expanding. Recent studies (e.g., Barrucand et al., 2007; Vargas et al., 2011; Magrin et al., 2014) have reported that the frequency of dry events was larger during the first half of the 20th Century, decaying during the

second half when a notorious positive trend in precipitation favored the expansion of agriculture towards the west onto once semi-arid regions. Several studies have shown increases in monthly rainfall and reduction in the number of dry spells during the 20th Century (Penalba and Vargas, 2008; Naumann et al., 2008; Vargas et al., 2011). Interestingly, other recent studies (e.g., Krepper and Zucarelli, 2010; Chen et al., 2010; Lovino et al., 2014) have suggested that the positive trend in monthly precipitation may have slowed down in the first decade of the 21st Century. If confirmed, such change could be reflected in more droughts.

The cold phase of ENSO (*La Niña*) is widely recognized as an important forcing for the onset and duration of extreme dry periods in SESA (Labraga et al., 2002; Penalba and Vargas, 2004; Silvestri, 2005; Barrucand et al., 2007; Vargas et al., 2011). Yet, the ENSO cold phase forcing alone does not always lead to intense droughts (Chen et al., 2010; Cavalcanti, 2012). As discussed by Seager et al. (2010) and Mo and Berbery (2011), the ENSO signal on SESA droughts becomes more intense and with a better-defined spatial shape when the cold ENSO phase is concurrent with a warmer than average North Tropical Atlantic. In addition to the remote forcings, regional and local factors may contribute to extreme event modulation once they are initiated (Mo and Schemm, 2008; Müller et al., 2014). The moisture transports and soil moisture conditions are all known to influence the events' duration and intensity. Not least, persistent atmospheric circulations, like those associated with blocking episodes, may hinder the development of precipitation systems during long periods. A documented case was the 1962 drought when a persistent and intense blocking anticyclone prevented the supply of warm and moist air from Brazil and the Atlantic Ocean leading to drought conditions over most of Argentina (Malaka and Nuñez, 1980).

This research aims to advance the understanding and impacts of dry episodes on wheat, corn, and soybean yields over Argentina's core crop region. Each crop has its phenology with different critical periods (when drought may significantly impact its growth). For this reason, it is essential to consider not only seasonal droughts but also those that center on the critical months. A drought climatology based on different indices is essential to identify features that the analysis of a single index might miss. This is the approach followed here. Our documentation focuses on drought frequency, duration, and severity and assesses its impacts on the crop yields. Section 2 presents the region of interest and describes the data and methods. The results and productivity indices are shown in Section 3. Discussion and conclusions are presented in Section 4.

2 Methods

2.1 Region of interest

Our analysis focuses on SESA (Fig. 1a) and more specifically in the region known as the Core Crop Region bounded by 36-29°S and 65-59°W (red box in Figs. 1b-d), where most (about 80%) of the Argentine production of wheat, corn, and soybean are found. The dark green color points out the regions where each crop's production is more intense. Values of production for

each crop are also shown in Figs. 1b-d. This region includes almost entirely the Provinces of Córdoba and Santa Fe, and part of the Provinces of Entre Ríos, Buenos Aires, La Pampa, Santiago del Estero, Corrientes (Provinces are identified in Fig. 1a).

Wheat, corn, and soybean have different life cycles that last about seven to nine months (lower bars in Figs. 1b-d). Wheat is planted during late austral fall or early winter (May-Jun) and harvested during summer. It is most sensitive to water availability during its growth period in spring (Oct-Nov). Planting of corn and soybean occurs in austral spring (Oct-Dec), and both are harvested in the fall. Their most sensitive period takes place during the summer, specifically Dec-Jan for corn and Jan-Feb for soybeans. Therefore, a year's crop production could be largely impacted even if a dry period lasting just one month or even less occurs during the critical growth period. While these are the crops' traditional cycles, it has become possible to have double-cropping at specific locations, i.e., have two crops with different cycles in one year by making the second cycle shorter. Crop rotation -which also has the advantage of reducing the need for fertilizers- introduces planting of corn or soybean right after the wheat harvest—the second crop results in smaller but still profitable production (Senigagliese, 2004).

2.2 Data sets and drought indices

This analysis of droughts focuses on precipitation (P), soil moisture (SM), and their derived standardized indices. Series of P and SM were turned into anomalies by removing their mean annual cycle. The monthly precipitation data covers 40 years, from January 1979 to December 2018, and was developed by NCEP's Climate Prediction Center (CPC). It consists of in situ observations spatially interpolated to a regular $0.5° \times 0.5°$ latitude-longitude grid cell (Chen et al., 2008). This product has been used as a benchmark for model evaluation in South America (Silva et al., 2011). In the absence of soil moisture observations, we employ products obtained from the Global Land Data Assimilation System (GLDAS; Rodell et al., 2004; Meng et al., 2012; Beaudoing and Rodell, 2019; 2020). GLDAS uses several land surface models to derive soil moisture from the surface water and energy balances forced by observations. The Noah Model is considered here. It has four soil layers (0-10 cm, 10-40 cm, 40-100 cm, and 100-200 cm) totaling 2 meters depth (Rodell et al., 2004). The total soil moisture in a column is the sum of the content in the four layers. The soil moisture data set consists of monthly values at a spatial resolution of $0.25° \times 0.25°$ over the same period of analysis as precipitation. Evaluation of GLDAS soil moisture products in the Humid Pampas was recently performed by Grings et al. (2015) and Spennemann et al. (2015; 2020). According to Grings et al. (2015), GLDAS is a good soil moisture benchmark in the Pampas region since it achieved the highest correlation ($r > 0.80$) with in situ soil moisture measurements. Spennemann et al. (2015, 2020) also reported that GLDAS reproduces soil moisture observational patterns satisfactorily. They also found that GLDAS products can be used as soil monitoring indices in agricultural production management.

Several drought indices have been defined to characterize droughts. The World Meteorological Organization (WMO) recommends selecting a particular index depending on the data available and ease of application (Byakatonda, 2018). It also recognizes the Standard Precipitation Index (SPI) advantages to study meteorological droughts (Hayes et al., 2011). SPI

represents a standardized precipitation anomaly and stands among the most used indices to quantify and monitor droughts (Keyantash and Dracup, 2002; Mishra et al., 2009; Hayes et al., 2011). In addition to the SPI or any precipitation index, other environmental variables may need to be included depending on the study region's characteristics and climate (e.g., Byakatonda, 2018). Soil moisture is particularly useful in agricultural areas, as they reflect the water content in the upper part of the soil where crops grow. Then, we used the standard indices SPI for precipitation and SSI for soil moisture (McKee et al., 1993; 1995; Hao and AghaKouchak, 2014; Hao et al., 2014).

SPI and SSI were computed following Hao and AghaKouchak (2014) approach and Farahmand and AghaKouchak (2015), which allows obtaining non-parametric standardized indices for many climate variables. A growing body of research attests that a non-parametric approach is better than a parametric one for studies of droughts. Unlike parametric approaches, non-parametric methods do not rely on any theoretical distribution. Parametric and non-parametric (empirical) probability density functions tend to have differences in the tails, where the parametric distribution may not be a good fit (Farahmand and AghaKouchak, 2015). A comparison of parametric and non-parametric estimates of SPI (Soláková et al., 2014) found that differences can be significant in terms of drought severity and not as much in terms of duration. According to Mallenahalli (2020), the non-parametric SPI can better categorize the drought classes, representing better the extent of dryness and normality conditions than parametric approaches. For these reasons, we adopted a non-parametric methodology that uses an empirical function (Gringorten, 1963; Farahmand and AghaKouchak, 2015). This method circumvents the use of theoretical functions, avoids issues with zero precipitation values, and is suitable in precipitation and soil moisture studies. Lastly, it is also an opportunity to provide a different approach in the index construction that has not been tested yet in the region.

The SPI and SSI were calculated following a non-exceedance empirical probability function for extreme events (Gringorten, 1963).

$$p(x_i) = \frac{i - 0.44}{n + 0.12},$$
(1)

Equation 1 represents the associated probability of non-exceedance for the *ith* element of the series, where *x* is either P or SM, *i* is the rank of non-zero values of the sample, and *n* is the size of the sample. This probability is then transformed into Standardized Indices (*SI*), applying the inverse of the standard normal distribution function ($\emptyset$) to the results of $p(x_i)$ (Farahmand and AghaKouchak, 2015) as follows:

$$SI = \emptyset^{-1}\left(p(x_i)\right),$$
(2)

This approach is applied to precipitation and soil moisture to create the corresponding indices, SPI and SSI.

Here, SPI and SSI are defined for two different time scales, three and six months, to facilitate monitoring meteorological and agricultural droughts. SPI3 (values for SPI at 3-months scale) reflect wet or dry conditions for short and medium time ranges and estimate the climate conditions at critical stages of the crops' growth. SPI6 provides information between seasons and can

be a reference point of the start of the anomalous behavior of flows and reservoir levels, which usually have larger time scales than precipitation itself. As defined by soil moisture content, the less variable SSI index can identify and monitor more directly seasonal agricultural droughts (Hao et al., 2014). While SPI is widely used for drought monitoring and prediction, SSI produces a reliable representation of drought persistence (Farahmand and AghaKouchak, 2015).

The time series of wheat, maize and soybean yields cover the seasons 1979/80 to 2018/2019 for the provinces of Santa Fe and Córdoba, covering most of the Core Crop Region (see Fig. 1d). Data are available from the Ministry of Agriculture, Livestock, and Fisheries (MAGyP, 2020).

2.3 Definitions and approach

A drought is a sustained period of below-normal water availability (Tallaksen and Van Lanen, 2004; Van Loon, 2015). Droughts are identified as "meteorological droughts" when there is a precipitation deficit over a period of time. A continued precipitation deficit can lead to a scarcity of soil moisture that does not meet the plants' water demand. In this case, the drought is called "agricultural drought". This study focuses on meteorological and agricultural droughts and their impacts on crop yields within the region of interest.

For this analysis, droughts are defined as those periods when SPI or SSI depart from the mean at least by minus one standard deviation. Drought events below that threshold range from moderate to extreme droughts (McKee et al., 1995). Weaker or milder droughts were estimated using a threshold of one-half the standard deviation. Droughts persist as long as they continue to exceed the threshold. We also examined different periods, starting at one month and more prolonged. We included the one-month results in Fig. 6 for completeness, but most of our analysis and conclusions are based on longer periods.

Low-frequency variability modes in the drought indices were identified using a Singular Spectrum Analysis (SSA) approach (Ghil et al., 2002; Wilks, 2006). SSA decomposes the time series in temporal-empirical orthogonal functions (T-EOFS) and temporal-principal components (T-PCS) and facilitates the interpretation of processes related to interannual modes of climate variability and the cases of drought. The SSA was used to identify the nonlinear trends and interannual quasi-oscillatory modes. Following Von Storch and Navarra (1995), we choose a window length (W) of 120 months as it does not exceed one-third of the length of the whole period and resolves quasi-periods in the interannual band 1 year < T < 10 years.

Dry events were analyzed by studying their frequency, duration, severity, and areal extent. Drought frequency (F) indicates the percentage of droughts during the time of analysis with respect to the total possible cases, in scales of months or the critical months periods for crop growth. Therefore, the frequency analysis is performed at monthly steps for the whole period and for each crop's critical periods. The frequency distribution of drought events also depends on the duration (D), that is, the length in time an index remains below the threshold until it reaches again. The drought magnitude is defined as the average deficit of

195 an index during the duration of the event. The drought severity (S) is equivalent to the accumulated water deficit on the event (Dracup et al., 1980), and it is defined as the magnitude times the duration, i.e., $S = D \times M$ (see Yevjevich, 1967; Keyantash and Dracup, 2002). The properties of frequency, duration, and severity of droughts are unique to the thresholds that define them. The analysis is completed with the examination of the droughts' areal extent (A).

200 An analysis of the relation between drought occurrence and annual crop yields of wheat, corn, and soybean is performed for Santa Fe and Córdoba. First, crop yield data were detrended to remove the increasing yields resulting from technological and genetic improvements. The detrended series can be better related to drought characteristics. Then, we examined the Pearson correlation coefficients between the annual detrended crop yields and the drought indices values for critical crop months (ON for wheat, DJ for corn, and JF for soybean).

205 **3 Results**

3.1 Droughts in the core crop region

3.1.1 Spatial analysis

Figure 2 presents the spatial distribution of the percentage of months under moderate to extreme drought conditions for northern Argentina as characterized by SPI1, SPI3, SPI6, and soil moisture anomalies. The occurrence of drought in
210 northeastern Argentina ranges between 12% and 14% for SPI1 (Fig. 2a), while months with droughts seem to increase up to 18% as characterized by SPI3/6 (Figs. 2b and 2c). Soil moisture anomalies show that droughts are distributed mainly in the north of Argentina, with about 16% - 18% of months with drought. Droughts, as characterized by SPI1/3/6 (Figs. 2a-c), reveal a homogeneous spatial distribution and an increasing drought percentage as with the time scale of the indicator. In contrast, the spatial pattern of soil moisture anomalies shows a decrease in drought percentages for arid regions (Fig. 2d). Inside the
215 Core Crop Region, droughts are more frequent towards the north, with percentages of months under moderate to extreme drought conditions from 14% to 16% for SPI1/3 (see Figs. 2a-b). Fig. 2d indicates that months with drought conditions, as represented by SPI6, are equivalent to 18% towards the region's north and southwest. Conversely, drought presence declines towards the southeastern core crop region as all SPI, and SM show percentages descend to 12% (Figs. 2a-d).

220 The drought's occurrence during the crops' critical growing periods provides valuable information for decision making. Crops have a stage during growth when they become more sensitive to water availability, and this changes with the type of crop. Spring and summer represent the most critical seasons in terms of the crops' critical months. For instance, the crucial period for wheat occurs in late spring (October and November). For corn, it is during the summer (December and January) and even later for soybean (January and February). Therefore, Figure 3 presents the spatial distribution of the percentage of months
225 under moderate to extreme drought conditions characterized by SPI during the corresponding critical months for each crop.

The three crop types present many areas where drought conditions are 18% or higher. Figures 3a-c show that shorter-duration droughts characterized by SPI3 tend to be more common towards the west of the region, affecting corn and soybean crops particularly. Figures 3d-f show that longer duration droughts, as represented by SPI6, have a probability of 18% over all the Core Crop Region but mainly during corn and soybean critical months. These results suggest that droughts over the core crop region are more frequent during summer months than during spring, affecting the corn and soybean critical periods more than the wheat's critical period.

3.1.2 Temporal variability

Figure 4 presents the time series of SPI1, SPI3, SPI6, and soil moisture anomalies, area-averaged over the Core Crop Region. SPI indices and soil moisture (Figs 4a-d) help identify wet and dry periods and their interannual variability. Notably, as the SPI time scale increases (from one month to six months), the variability is reduced (see Figs. 4a and 4c). Soils function as a physical filter because the output signal (soil moisture) has a lower frequency variability than the input precipitation. The reason is that the time it takes for the precipitated water to infiltrate the soil and move through deeper layers has a dampening or smoothing effect that Entekhabi et al. (2006) described as a low-pass filter.

The main features in Fig 4 are summarized in Table 1 that reveals the dominant modes of interannual variability for SPI1, SPI3, SPI6, and soil moisture. They are (i) a trend, (ii) a band with decadal periodicities, and (iii) a band close to 2.3 years periodicities. Trends explain different percentages of the total variability of the series. Interannual modes in both bands can explain 35% of the total variability of the SPI6 series and 37% of the soil moisture variability. Decadal cycles in SPI and soil moisture series are closely related and reflect the dry periods of 1987-1991, 1994-1999, and 2004-2013 (see Figs. 4a-d). The short-term 2.3-year cycle of interannual variability is evidenced by frequent wet and dry events between 2000 and 2018 (see Fig. 4b-d). Interestingly, higher amplitudes are noticed starting around 2000. This result agrees with Lovino et al. (2018a, b), who suggested that short-term variability (2.5- to 4-year periods) in precipitation exhibits a large increase in amplitude after 2000.

3.1.3 Frequency distribution

Figure 5 presents histograms of precipitation and soil moisture anomalies that were prepared to analyze the distribution of wet and dry periods over the Core Crop Region. As we are dealing here with anomalies, a right-skewed histogram indicates more cases of water deficit conditions than water excess conditions, while a left-skewed histogram indicates the opposite. The kurtosis, in addition, reflects the propensity to produce outliers (Westfall, 2014). The precipitation and soil moisture anomalies display right-skewed histograms (Fig. 5a) with different kurtosis. This result indicates that drought episodes are more common than wet events over the region. The precipitation histogram (blue, hatched) exhibits extreme events that are related to a higher kurtosis (see inset in Fig. 5a) and heavy-tailed distribution (Westfall, 2014). The soil moisture histogram shows a more compact distribution with low kurtosis and light-tailed histograms. This indicates that weak water deficit events are more frequent (e.g.,

about 150 events are found in the range -10 to 0 mm). On the other hand, a wider departure from the mean for precipitation histogram indicates that extreme dry events may occur although their frequency is low, revealing, on the one hand, the need to use multiple indices and, on the other, the complexity of their simultaneous interpretation.

To better understand the seasonal distribution of dry events inside the Core Crop Region, seasonal boxplots were built for precipitation and soil moisture anomalies (Figs. 5b-c). The use of anomalies leads to an average of 0, while the median is slightly negative following the skewed histograms in Fig. 5a. Precipitation plots in Fig. 5b present the widest distribution during summer (DJF), followed by autumn (MAM) and spring (SON). For each season, boxplot lower and upper whiskers stand for the 5th and 95th percentiles; values outside whiskers (i.e., below the 5th percentile or above the 95th percentile) represent the outliers. The figure shows that the more extreme dry events can happen during summer and autumn, with outliers reaching -100 mm. By contrast, during winter (JJA) most of the values are found near 0 mm with small deviations: outliers around -25 mm indicate that this region's events are not necessarily extreme.

Boxplots for soil moisture in Fig. 5c show that seasonal distributions are more uniform, probably due to their lower variability and lower range values than precipitation. Interestingly, the outliers have the largest magnitudes during autumn (MAM), reaching deviations between -20 and -30 mm. This result is consistent with a delay with respect to precipitation, which showed the most extreme cases during summer (DJF). The delay also results in that soil moisture exhibits more extreme cases during winter (JJA), following the large values for precipitation during autumn (MAM).

3.1.4 Drought duration

Drought duration is defined as the number of months that a given drought index (SPI and SSI) exceeds a certain threshold, X_i. For both SPI and SSI, the value $X_1 = -0.5$ identifies mild to extreme droughts, while using $X_2 = -1$ detects moderate to extreme droughts. Figure 6 shows the SPI and SSI frequency of droughts inside the Core Crop Region regarding different events' durations, expressed in months. Each histogram presents the number of events for each duration, hinting at different types of droughts.

All histograms in Fig. 6 present a common pattern with a higher frequency for short-term events (1-3 months). The frequency (or the number of cases) declines as drought duration increases. These results suggest that long-term droughts, particularly beyond seven months, are uncommon inside the Core Crop Region. Table 2 presents the percentages of drought occurrence for short-term droughts and more prolonged than three months events as characterized by SPIs and SSI at time scales of 3 and 6 months. The SPI indices have more ability to identify short-lived droughts than the standardized index based on soil moisture. In contrast, SSI seems a better fit to detect more prolonged droughts (see Table 2). In summary, short-term droughts are better represented by an index like SPI, with higher variability and a short time scale. Long-term drought events are more easily detected with an index of lower variability and a higher time scale.

3.1.5 Severity and spatial extent of droughts

Drought duration and magnitude are essential to describe droughts, as well. It is central to have a measure of severity and spatial extent of the drought. Severity can be defined as the product between the drought duration and drought magnitude. A drought's spatial extent refers to the area that exceeds a certain threshold (e.g., X_2), and it is expressed as a percentage of the total Core Crop Region. Figure 7 presents the time series of severity and spatial extent computed from SPIs and SSIs for the Core Crop Region. According to Figs. 7a-b, the most severe droughts occurred during 1988/89, 1995/96, 2008/2009, and the last one during 2017/2018, consistently with the analysis in Fig 4. Time series of drought severity are negative because they result from the product of a negative drought magnitude (defined by using a negative threshold like X_2) and a positive duration. Severity indices seem to be greater in magnitude (more negative) when computed from 6-month time scales (SPI6 and SSI6), which is due to a lesser index variation as the time aggregation of the index increases.

The Core Crop Region extends over 500,000 km^2 in Argentina's center (shown in Fig. 1). Figs. 7a and 7c suggest that the more severe droughts are also the ones with a greater spatial extent within this area. Further, for every severe event, the SPI time series indicate that droughts are extended around 80 to 90% of the core crop region, increasing these events' impacts on the region's main activities. Even droughts that are not quantitatively as severe can spread almost in equal proportions as the severe ones; for instance, the shorter droughts detected by SPI3 in 1996, 2002, 2006, and 2012 spread through 60% to 80% of the core crop region (see red lines in Fig. 7c). The soil moisture's lower variability results in similar time series of SSI3 and SSI6 (Figs. 7b, d) that have a high ability to identify drought events with increased severity and large spatial extension. Our results suggest that both SPI and SSI can identify severe droughts, but they have subtle differences. SPI is useful to detect a drought's extension, being it severe or not. On the other hand, SSI tends to filter out non-severe droughts, offering a cleaner representation of the more extended severe cases.

3.2 Crop yields in the core crop region

Due to the importance for regional economies, it is always of interest to stress the droughts' negative impact on crops. Changes in crop yield, defined as crop production per unit area (kg ha^{-1}), reflect not only the effects of climate variability but also non-climatic factors like technological and biotechnological advances (including seed quality, different use of fertilizers, sawing or harvesting dates), usually in the form of a positive nonlinear trend. This can be noticed in Fig. 8, which presents the 1979-2018 area-averaged time series of corn, wheat, and soybean yields for the provinces of Santa Fe and Córdoba. The wheat and soybean trends show a significant change around the mid-1990s, whereas, for corn, a change occurred earlier in the late 1980s. On average, wheat and soybeans yields increased from 1,000 to 3,000 kg ha^{-1} (Figs. 8a and 8c) while corn yield increased from 3,000 to almost 8,000 kg ha^{-1} (Fig. 8b). As stated, at least most of the increases may be due to advances in the production process. These trends should be removed when examining the crop yield variability and its relation to droughts. Crop yield time series were fitted with a cubic polynomial trend (see dotted lines in Figs. 8a-c). Then, the trends were subtracted from the

original series, leaving the shorter-term variability (see Figs. 8d-f). Detrended time series of one or more crop yields exhibit the largest negative anomalies concurrently with the most severe droughts identified by SPI6 and soil moisture anomalies (Figs. 4c and 4d) recorded in 1988/1989, 1995/1996, 2008/2009, and 2017/18 (Figs. 8d-f). Not all crops are affected equally by drought as slight differences in the onset of the drought and the crops' critical growth periods may affect them differently.

Table 3 presents the correlation coefficients between detrended crop yields and SPI/SSI during the crops' critical periods. The results suggest a direct relation between summer crops (corn and soybean) and deficits in precipitation and soil moisture during both crops' critical periods. Of the three crops, wheat yields have the lowest correlations with the indices. Table 3 also shows that the shorter-scale indicators (SPI3 and SSI3) achieve a better correlation with crop yields than the longer-scale indicators (SPI6 and SSI6), making them a good descriptor of crop yield losses.

Figure 8d-f shows that large negative anomalies of detrended corn and soybean yields (Figs. 8e and 8f) are consistent with the lowest values of SPI3 during the drought events in 1988/1989, 1995/1996, and 2017/18 (Fig. 7). Severity, derived from SSI3 and SSI6, reached extreme negative values around -8 during the crops' critical growth period. Similarly, a considerable reduction in wheat production in 2009 is related to large (negative) drought severity values, particularly for the Santa Fe Province (see blue line in Fig. 8d). Although with some differences in the anomaly values, the detrended series of corn and soybean yield are in phase and exhibit a close resemblance (Figs. 8e and 8f). Increases and decreases in production take place nearly simultaneously, unlike the behavior with wheat (Fig. 8d). Both crops present significant yield losses approximately in the years of major droughts (see Fig. 7). This could be related to the one-month overlap during both sensitive periods, as the two crops have January as a common month during their critical growth in summer.

The detrended time series (Fig. 8d-f) show declines in production due to major drought events. The losses in production may reach up to 1500 kg ha^{-1} for corn and between 500 to 1000 kg ha^{-1} for wheat and soybean. Correlations between SPI3 and the different crop yields (Table 3) suggest that corn and soybean are more sensitive to water availability. Figs. 8e and 8f show that SPI3 values and crop production have a better representation with a detrended series of corn and soybean yields. Notably, a good fit is observed for the most severe drought events in 1988/1989, 1995/1996, and 2017/2018. Conversely, from 1998 to 2007, no severe events occurred (see Fig. 7a and 7b). For those years, crop production ranges from neutral to positive values, with a maximum for corn in Córdoba. However, in this period without severe droughts, a drop in Córdoba' soybean yield occurred in 2004 that is correlated with a moderate drought represented by an SPI close to -1.2 during the soybean's critical period. This could imply that SPI3 may be used as a drought indicator also during moderate drought events. We have not discussed the compound effect of water scarcity and heat waves, which may intensify crop yield losses. Llano and Vargas (2016) suggested that the compound event of precipitation and maximum temperature in corn sensitive growing period have the greatest influences on crop production in central-eastern Argentina.

4 Discussion and conclusions

This study documents droughts in Argentina's Core Crop Region, a region where wheat, corn, and soybean production is the most abundant. The investigation is based on the analysis of precipitation and soil moisture analysis, and their derived indices SPI and SSI, respectively, at different time scales. The drought properties that were examined include magnitude, duration, severity, and areal extension. The analysis was completed by examining the relationship between drought properties and crop yields. Droughts were identified as events with a water shortage exceeding one standard deviation or more of the mean values. The requirement was slightly relaxed for estimating the duration of events, considering water deficits that depart at least half a standard deviation. The analysis was performed at different time scales: all months and monthly for each crop's critical growing months. Crop yields have increased through the years due to more beneficial climate conditions, but more importantly, thanks to agro-technological advancements. We inspected drought impacts on crop yield after removing those trends.

Our results indicate that the drought's occurrence percentage depends on whether SPI or SM anomalies are used, as the standardized nature and time aggregation of the SPI index tends to emphasize longer time scales. Short-term droughts are more easily detected when using an index with higher variability and a short time scale. For this reason, short-term drought-prone regions and their relation to seasonality within the core crop region are better identified using SPI1 and SPI3. The presence of long-term events is more readily recognized with an index of lower variability and at lower time scales.

Spatial patterns of drought's occurrence percentage for all times considered do not show clear features. The drought's occurrence percentage in northeastern Argentina ranges between 12-18% depending on the drought indicator and location, with the larger values found towards the Core Crop region's eastern/northeastern sector. The drought's percentage of occurrences, based on soil moisture anomalies, shows a second area of slightly high values for the semi-arid climate towards the wore Crop Region's western portion. During summer, droughts affect corn and soybean production, mainly towards the west and center of the Core Crop Region.

Soil moisture acts as a temporal filter because it smooths out the highly variable precipitation resulting in a lower frequency signal. Similarly, the SPI time series variability is reduced when the time scale increases from one month to six. Frequency analysis for different durations indicates that short-term droughts are more common than long-term droughts. Our findings show that values accumulated for 1-3 months account for about 78-88% of the events depending on the threshold and variable considered. A few can extend up to one year and even fewer even longer. However, if a multi-year drought experienced breaks, each period would be regarded as a separate case. These results are consistent with drought frequency values found by Minetti et al. (2007), who reported that similar 1-3 months events account for 90% of the Argentine Humid Pampa cases. Small differences could be related to the use of different indices and thresholds in the definition of drought. In general, long-term drought events are more easily detected with an index of lower variability, like SSI and a higher time scale.

390   The timing of droughts is central to their impact on crop yields. The reason is that the crops' fastest growth during the critical periods is highly susceptible to water availability. Even a short-duration dry event, if concurrent with the critical growth period, may significantly impact crop performance. Large drought severity values taking place during sensitive months will result in significant crop yield losses. Suppose a severe drought event is identified and quantified during the crop-sensitive months. In that case, the drought indicator can be helpful as a warning that crop yields can be expected to be lower, potentially resulting

395   in significant economic losses. Our results suggest that the shorter-scale indicators (SPI3 and SSI3) during crop critical periods are most appropriate to predict crop yield losses than the longer-scale indicators (SPI6 and SSI6).

Argentine agriculture has benefited from the increased use of fertilizers, agrochemicals, and the management of genetically modified crops, leading to important positive trends in crop yields. Removing those trends facilitates contrasting of year-to-

400   year yield variability and climate variations. Previous studies have partially addressed the relationship between droughts and losses on crop yields (e.g., Podestá et al. 2009; Holzman et al., 2014; Jozami et al., 2018). Our study advances the topic by providing a novel severity analysis and quantifying the link between detrended crop yield and drought indicators (SPI/SSI) during crop critical periods. Wheat yields have the lowest correlations with drought indices. On the other hand, our results suggest a direct relation between corn and soybean yields and deficits in precipitation and soil moisture during both crops'

405   critical periods. Corn seems to be the most sensitive summer crop to water deficit in terms of crop productivity. As a note of caution, corn production may be affected by water availability and temperature and geographical adaptation (Butler and Huybers, 2013). These two features have not been addressed here.

Data availability

CPC precipitation and GLDAS soil moisture data sets are available at NWS, CPC, https://doi.org/10.1029/2007JD009132,

410   Chen et al., 2008; and GLDAS, https://doi.org/10.5067/9SQ1B3ZXP2C5, Beaudoing and Rodell, 2019; https://doi.org/10.5067/SXAVCZFAQLNO, Beaudoing and Rodell, 2020. Crop yields data sets are provided by MAGyP, available at http://datosestimaciones.magyp.gob.ar/reportes.php?reporte=Estimaciones.

Author contribution

The author and co-authors contributed to the design and implementation of the research, to the analysis of the results, and to

415   the writing of the manuscript.

Competing interests

The authors declare that they have no conflict of interest.

Acknowledgments

The authors would like to thank the reviewers for their thoughtful comments that improved the manuscript. This research was
420 carried out with the support of Projects CRN3035 and CRN3095 of the Inter-American Institute for Global Change Research (IAI), supported by the US National Science Foundation. NOAA Grant NA19NES4320002 (Cooperative Institute for Satellite Earth System Studies, CISESS) and Project IO-2017-00254 of the Ministry of Science, Technology, and Productive Innovation of Santa Fe (Argentina) are also acknowledged.

References

425 Ameghino, F.: Las secas y las inundaciones en la Provincia de Buenos Aires. Obras de retención y no de desagüe. Ministerio de Asuntos Agrarios de la Provincia de Buenos Aires, 5-62, 1884 (in Spanish).

Barrionuevo, A.: In Parched Argentina, worries over economy grow, New York Times, available at https://www.nytimes.com/2009/02/21/world/americas/21argentina.htm, last access: 21 April 2020, 2009.

Barrucand, M. G., Vargas, W. M., and Rusticucci, M. M.: Dry conditions over Argentina and the related monthly circulation
430 patterns. Meteorol. Atmos. Phys., 98, 99-114, https://doi.org/10.1007/s00703-006-0232-5, 2007.

Beaudoing, H., and Rodell, M.: GLDAS Noah Land Surface Model L4 monthly 0.25 x 0.25 degree V2.0, Greenbelt, Maryland, USA, Goddard Earth Sciences Data and Information Services Center (GES DISC), NASA/GSFC/HSL, Accessed: [12 March 2019], https://doi.org/10.5067/9SQ1B3ZXP2C5, 2019.

Beaudoing, H., and Rodell, M.: GLDAS Noah Land Surface Model L4 monthly 0.25 x 0.25 degree V2.1, Greenbelt, Maryland,
435 USA, Goddard Earth Sciences Data and Information Services Center (GES DISC), NASA/GSFC/HSL, Accessed: [12 March 2019], https://doi.org/10.5067/SXAVCZFAQLNO, 2020.

Butler, E. E., and Huybers, P.: Adaptation of US maize to temperature variations. Nat. Clim. Change, 3, 68, https://doi.org/10.1038/nclimate1585, 2013.

Byakatonda, J., Paridaa, B. P., Moalafhib, D. B., Kenabathob, Piet K.: Analysis of long-term drought severity characteristics
440 and trends across semi-arid Botswana using two drought indices. Atmos. Res., 213, 492-508, https://doi.org/10.1016/j.atmosres.2018.07.002, 2018.

Cavalcanti, I. F. A.: Large scale and synoptic features associated with extreme precipitation over South America: A review and case studies for the first decade of the 21st Century. Atmos. Res., 118, 27-40, https://doi.org/10.1016/j.atmosres.2012.06.012, 2012.

445   Chen, M., Shi, W., Xie, P., Silva, V., Kousky, V. E., Wayne Higgins, R., and Janowiak, J. E.: Assessing objective techniques for gauge-based analyses of global daily precipitation. J. Geophys. Res., 113, D04, https://doi.org/10.1029/2007JD009132, 2008.

Chen, J. L., Wilson, C. R., Tapley, B. D., Longuevergne, L., Yang, Z. L., and Scanlon, B. R.: Recent La Plata basin drought conditions observed by satellite gravimetry, J. Geophys. Res., 115, D22, https://doi.org/10.1029/2010JD014689, 2010.

450   Dracup, J. A., Lee, K. S., and Paulson, E. G.: On the definition of droughts. Water Resour. Res., 16, 297–302, https://doi.org/10.1029/WR016i002p00297, 1980.

Entekhabi, D., Rodriguez-Iturbe, I., Castelli, F.: Mutual interaction of soil moisture state and atmospheric processes. Journal of Hydrology, 184(1-2), 3-17. https://doi.org/10.1016/0022-1694(95)02965-6, 2016.

Farahmand, A., and AghaKouchak, A.: A generalized framework for deriving non-parametric standardized drought indicators.

455   Adv. Water Resour, 76, 140-145, https://doi.org/10.1016/j.advwatres.2014.11.012, 2015.

Ghil, M., Allen, M. R., Dettinger, M. D., Ide, K., Kondrashov, D., Mann, M. E., Robertson, A., Saunders, A., Tian, Y., Varadi, F., and Yiou, P.: Advanced spectral methods for climatic time series. Rev. Geophys., 40, 1-41, https://doi.org/10.1029/2000RG000092, 2002.

Gringorten, I. I.: A plotting rule for extreme probability paper. J. Geophys. Res., 68, 813-814,

460   https://doi.org/10.1029/JZ068i003p00813, 1963.

Grings, F., Bruscantini, C. A., Smucler, E., Carballo, F., Dillon, M. E., Collini, E. A., Salvia, M., Karszenbaum, H.: Validation strategies for satellite-based soil moisture products over Argentine Pampas. IEEE Journal of Selected Topics in Applied Earth Observations and Remote Sensing, 8(8), 4094-4105, DOI: 10.1109/JSTARS.2015.2449237, 2015.

Hao, Z., and AghaKouchak, A.: A non-parametric multivariate multi-index drought monitoring framework. J. Hydrometeorol.,

465   15, 89-101, https://doi.org/10.1175/JHM-D-12-0160.1, 2014.

Hao, Z., AghaKouchak, A., Nakhjiri, N., and Farahmand, A.: Global integrated drought monitoring and prediction system. Sci Data, 1, 140001. https://doi.org/10.1038/sdata.2014.1, 2014.

Hayes, M., Svoboda, M., Wall, N., and Widhalm, M.: The Lincoln declaration on drought indices: universal meteorological drought index recommended. Bull. Am. Meteorol. Soc., 92, 485-488, https://doi.org/10.1175/2010BAMS3103.1, 2011.

470   Holzman, M. E., Rivas, R., and Piccolo, M. C.: Estimating soil moisture and the relationship with crop yield using surface temperature and vegetation index. Int. J. Appl. Earth Obs. Geoinf., 28, 181-192, https://doi.org/10.1016/j.jag.2013.12.006, 2014.

International Monetary Fund (Eds): Primary commodities: Market developments and outlook, Commodities division research department, Washington DC, July 1990.

475   Jozami, E., Montero Bulacio, E. and Coronel, A.: Temporal variability of ENSO effects on corn yield at the central region of Argentina. Int. J. Climatol, 38: 1-12. https://doi.org/10.1002/joc.5154, 2018.

Keyantash, J., and J. A. Dracup.: The quantification of drought: An evaluation of drought indices. Bull. Amer. Meteor. Soc., 83, 1167–1180, https://doi.org/10.1175/1520-0477-83.8.1167, 2002.

Krepper, C.M., and Zucarelli, G.V.: Climatology of water excesses and shortages in the La Plata Basin. Theor Appl Climatol 102, 13–27, https://doi.org/10.1007/s00704-009-0234-6, 2010.

Labraga, J. C., Scian, B., and Frumento, O.: Anomalies in the atmospheric circulation associated with the rainfall excess or deficit in the Pampa Region in Argentina. J. Geophys. Res. D: Atmos., 107, 1-15, https://doi.org/10.1029/2002JD002113, 2002.

La Nación: La represa de Salto Grande dejaría de producir energía, available at: https://www.lanacion.com.ar/economia/la-represa-de-salto-grande-dejaria-de-producir-energia-nid591160, last access: 2 August 2019, 2004 (in Spanish).

Llano, M. P., and Penalba, O. C.: A climatic analysis of dry sequences in Argentina. Int. J. Climatol., 31, 504-513, https://doi.org/10.1002/joc.2092, 2010.

Llano, M.P., and Vargas, W.: Climate characteristics and their relationship with soybean and maize yields in Argentina, Brazil and the United States. Int. J. Climatol., 36: 1471-1483. https://doi.org/10.1002/joc.4439, 2016.

Lovino, M., García, N. O., and Baethgen, W. E.: Spatiotemporal analysis of extreme precipitation events in the Northeast region of Argentina (NEA). J. Hydrol.: Reg. Stud., 2, 140-158, https://doi.org/10.1016/j.ejrh.2014.09.001, 2014.

Lovino, M. A., Müller, O. V., Müller, G. V., Sgroi, L. C., and Baethgen, W. E.: Interannual-to-multidecadal hydroclimate variability and its sectoral impacts in northeastern Argentina. Hydrol. Earth Syst. Sci., 22, 3155–3174, https://doi.org/10.5194/hess-22-3155-2018, 2018a.

Lovino, M., Müller, O., Berbery, E. and Müller, G.: How have daily climate extremes changed in the recent past over northeastern Argentina? Global Planet. Change, 168, 78-97, https://doi.org/10.1016/j.gloplacha.2018.06.008, 2018b.

MAGyP: Ministry of Agriculture, Livestock and Fisheries of Argentina, monthly report May 2018, available at: https://www.magyp.gob.ar/sitio/areas/estimaciones/_archivos/estimaciones/180000_2018/180500_Mayo/180524_Informe%20Mensual%2024%2005%2018.pdf, last access: 18 September 2019. 2018 (in Spanish).

MAGyP: Ministry of Agriculture, Livestock and Fisheries of Argentina, https://www.agroindustria.gob.ar/sitio/areas/ss_mercados_agropecuarios/exportaciones, last access: 18 September 2019. 2019.

MAGyP: Ministry of Agriculture, Livestock and Fisheries: Agricultural Datasets (in Spanish), http://datosestimaciones.magyp.gob.ar/reportes.php?reporte=Estimaciones, last access: 24 October 2020.

Malaka, I., and Nuñez, S.: Aspectos sinópticos de la sequía que afectó a la República Argentina en 1962. Revista Geoacta, 10, 1-22, 1980 (in Spanish).

Magrin, G. O., Marengo, J. A., Boulanger, J.-P., Buckeridge, M. S., Castellanos, E., Poveda, G., Scarano, F. R., and Vicuña, S.: Central and South America, in: Climate Change 2014: Impacts, Adaptation, and Vulnerability. Part B: Regional Aspects. Contribution of Working Group II to the Fifth Assessment Report of the Intergovernmental Panel on Climate Change, edited by: Barros,V. R., Field, C. B., Dokken, D. J., Mastrandrea, M. D., Mach, K. J., Bilir, T. E., Chatterjee, M., Ebi, K. L., Estrada, Y. O., Genova, R. C., Girma, B., Kissel, E. S., Levy, A. N., MacCracken, S., Mastrandrea, P. R., and White, L. L., Cambridge University Press, Cambridge, United Kingdom and New York, NY, USA, 1499–1566, 2014.

Mallenahalli, N.K.: Comparison of parametric and non-parametric standardized precipitation index for detecting meteorological drought over the Indian region. Theor Appl Climatol 142, 219–236. https://doi.org/10.1007/s00704-020-03296-z, 2020.

McKee, T. B., N. J. Doesken, and J. Kleist.: The relationship of drought frequency and duration to time scales. Proceedings of the 8th Conference on Applied Climatology, Anaheim, CA, 17-22 January 1993, Amer. Meteor. Soc., 179-184. 1993.

McKee, T. B., N. J. Doesken, and J. Kleist.: Drought monitoring with multiple time scales. Proceedings of the 9th Conference on Applied Climatology, Dallas, TX, 15-20 January 1995, Amer. Meteor. Soc, 233-236. 1995.

Meng, J., R. Yang, H. Wei, M. Ek, G. Gayno, P. Xie, and K. Mitchell.: The Land Surface Analysis in the NCEP Climate Forecast System Reanalysis. J. Hydrometeorol., 13, 1621–1630, https://doi.org/10.1175/JHM-D-11-090.1, 2012.

Minetti, J. L., Vargas, W. M., Vega, B., and Costa, M. C.: Las sequías en la Pampa Húmeda: Impacto en la productividad del maíz. Revista Brasileira de Meteorología, 22, 218-232, https://doi.org/10.1590/S0102-77862007000200007, 2007.

Mishra, A.K., Singh, V.P. and Desai, V.R.: Drought characterization: a probabilistic approach. Stochastic Environ. Res. Risk Assess., 23, 41–55, https://doi.org/10.1007/s00477-007-0194-2, 2009.

Mo, K. C., & Schemm, J. E.: Relationships between ENSO and drought over the southeastern United States. Geophys. Res. Lett., 35(15), https://doi.org/10.1029/2008GL034656, 2008.

Mo, K. C., & Berbery, E. H.: Drought and persistent wet spells over South America based on observations and the US CLIVAR drought experiments., J. Clim., 24, 1801-1820, https://doi.org/10.1175/2010JCLI3874.1, 2011.

Müller, O. V., Berbery, E. H., Alcaraz-Segura, D., and Ek, M. B.: Regional model simulations of the 2008 drought in southern South America using a consistent set of land surface properties. J. Clim., 27, 6754-6778, https://doi.org/10.1175/JCLI-D-13-00463.1, 2014.

Naumann, G., Vargas, W. M., and Minetti, J. L.: Estudio de secuencias secas en la Cuenca del Plata: Implicancias con las sequías. Revista Meteorologica, 33, 65-81, 2008.

Naumann, G., Llano, M. P., and Vargas, W. M.: Climatology of the annual maximum daily precipitation in the La Plata Basin. Int. J. Climatol., 32, 247-260, https://doi.org/10.1002/joc.2265, 2012.

Penalba, O. C., and Vargas, W. M.: Interdecadal and interannual variations of annual and extreme precipitation over central-northeastern Argentina. Int. J. Climatol., 24, 1565-1580, https://doi.org/10.1002/joc.1069, 2004.

Penalba, O. C., Bettolli, M. L., and Vargas, W. M.: The impact of climate variability on soybean yields in Argentina. Multivariate regression. Meteorol. Appl., 14, 3-14, https://doi.org/10.1002/met.1, 2007.

Penalba, O. C., and Vargas, W. M.: Variability of low monthly rainfall in La Plata Basin. Meteorol. Appl., 15, 313-323, https://doi.org/10.1002/met.68, 2008.

Penalba, O. and M. P. Llano.: Contribución al estudio de las secuencias secas en la zona agropecuaria de Argentina. Revista Meteorologica, 33, 51-64, 2008 (in Spanish).

545 Podestá, G., Bert, F., Rajagopalan, B., Apipattanavis, S., Apipattanavis, S., Laciana, C., Weber, E., Easterling, W., Katz, R., Letson, D., Menendez, A.: Decadal climate variability in the Argentine Pampas: regional impacts of plausible climate scenarios on agricultural systems. Clim Res, 40:199-210, https://doi.org/10.3354/cr00807, 2009.

Rodell, M., Houser, P. R., Jambor, U., Gottschalck, J., Mitchell, K., Meng, C., Arsenault, K., Cosgrove, B., Radakovich, J., Bosilovich, M., Entin, J. K., Walker, J. P., Lohmann, D., and Toll, D.: The Global Land Data Assimilation System, Bull. Am.
550 Meteorol. Soc., 85, 381-394, https://doi.org/10.1175/BAMS-85-3-381, 2004.

Seager, R., Naik, N., Baethgen, W., Robertson, A., Kushnir, Y., Nakamura, J., and Jurburg, S.: Tropical oceanic causes of interannual to multidecadal precipitation variability in southeast South America over the past Century. J. Clim., 23, 5517-5539, https://doi.org/10.1175/2010JCLI3578.1, 2010.

Senigagliese, C.: Serie IDIA XXI: revista de información sobre investigación y desarrollo agropecuario. v. 4, no. 6, 72-75,
555 2004.

Siebert, S., Henrich, V., Frenken, K., and Burke, J.: Update of the digital global map of irrigation areas to version 5. Rheinische Friedrich-Wilhelms-Universität, Bonn, Germany. FAO, 151 pp., 2013.

Silva, V. B., Kousky, V. E., Higgins, R. W.: Daily precipitation statistics for South America: An intercomparison between NCEP reanalyses and observations. Journal of Hydrometeorology, 12(1), 101-117, https://doi.org/10.1175/2010JHM1303.1,
560 2011.

Silvestri, G. E.: Comparison between winter precipitation in southeastern South America during each ENSO phase. Geophys. Res. Lett., 32(5), https://doi.org/10.1029/2004GL021749, 2005.

Soláková T, De Michele C, Vezzoli R.: Comparison between parametric and non-parametric approaches for the calculation of two drought indices: SPI and SSI. J Hydrol Eng 19(9):04014010, https://doi.org/10.1061/(ASCE)HE.1943-5584.0000942,
565 2014.

Spennemann, P. C., Rivera, J. A., Saulo, A. C., Penalba, O. C.: A comparison of GLDAS soil moisture anomalies against standardized precipitation index and multisatellite estimations over South America. Journal of Hydrometeorology, 16(1), 158-171, https://doi.org/10.1175/JHM-D-13-0190.1, 2015.

Spennemann, P. C., Fernández-Long, M. E., Gattinoni, N. N., Cammalleri, C., Naumann, G.: Soil moisture evaluation over
570 the Argentine Pampas using models, satellite estimations and in-situ measurements. Journal of Hydrology: Regional Studies, 31, 100723, https://doi.org/10.1016/j.ejrh.2020.100723, 2020.

Tallaksen, L. M., & Van Lanen, H. A. (Eds.).: Hydrological drought: processes and estimation methods for streamflow and groundwater (Vol. 48), Elsevier, 2004.

Van Loon, A. F.: Hydrological drought explained. Wiley Interdisciplinary Re-views: Water, 2(4), 359-392.
575 https://doi.org/10.1002/wat2.1085, 2015.

Vargas, W. M., Naumann, G., and Minetti, J. L.: Dry spells in the River Plata Basin: an approximation of the diagnosis of droughts using daily data. Theor. Appl. Climatol., 104, 159-173, https://doi.org/10.1007/s00704-010-0335-2, 2011.

Von Storch, H. and Navarra, A. (Eds.): Analysis of Climate Variability, Springer-Verlag, Berlin, Heidelberg, Germany, 334 pp., 1995.

580 Webber, J.: Argentina's drought: counting the costs, Financial Times, available at: https://www.ft.com/content/f7fd1da9-9848-39bc-9e15-168d0bd14dd7, last access: 27 March 2018.

Westfall, P. H.: Kurtosis as peakedness, 1905–2014. RIP. The American Statistician, 68, 191-195, https://doi.org/10.1080/00031305.2014.917055, 2014.

Wilks D. S.: Statistical Methods in the Atmospheric Sciences, Second Edn., International Geophysicis Series, Vol. 91, Elsevier

585 Inc, 627 pp., 2006.

Yevjevich, V. M.: Objective approach to definitions and investigations of continental hydrologic droughts, An. Hydrology papers (Colorado State University); no. 23. 1967.

	SPI1	SPI3	SPI6	SM Anomalies
Trend	-	3.2	5.5	-
Quasi-cycle, T ~ 10 yr	5.9	13.9	22	25.4
Quasi-cycle, T ~ 2.3 yr	-	7.8	13	11.6

590

Table 1: Percentage of variance explained by the dominant modes of interannual variability detected using SSA with a window length of 120 months. Computations were done over SPI1, SPI3, SPI6, and soil moisture anomalies from January 1979 to December 2018 in Core Crop Region.

	Duration [1-3 months]		Duration [>3 months]	
	(X_1)	(X_2)	(X_1)	(X_2)
SPI3	77.8	88.2	22.2	11.8
SPI6	68.7	76.7	31.3	23.3
SSI3	46.7	49.9	53.2	50.1
SSI6	38.5	44.0	61.5	56.0

595 **Table 2: Frequency of droughts for different durations, expressed as a percentage of the total drought events in Core Crop Region, from indices SPIs and SSIs. Droughts were detected using threshold X_1 (one half standard deviation) and X_2 (one standard deviation) from January 1979 – December 2018. The duration of the events was grouped into short-term [1-3 months] and long-term droughts [>3 months].**

Province	Crop	Indices			
		SPI3	SPI6	SSI3	SSI6
	wheat	0.15	0.05	0.17	0.15
Santa Fe	corn	0.67	0.58	0.58	0.40
	soybean	0.68	0.58	0.62	0.52

Province	Crop	Indices			
		SPI3	SPI6	SSI3	SSI6
	wheat	0.49	0.04	0.44	0.38
Córdoba	corn	0.60	0.55	0.51	0.55
	soybean	0.73	0.70	0.58	0.70

Table 3: Correlation Coefficients of the annual detrended crop yield and the maximum or minimum index value for critical crop months (ON for wheat, DJ for corn, and JF for soybean). Maximum or minimum index values are identified according to whether detrended annual crop yields are negative or positive.
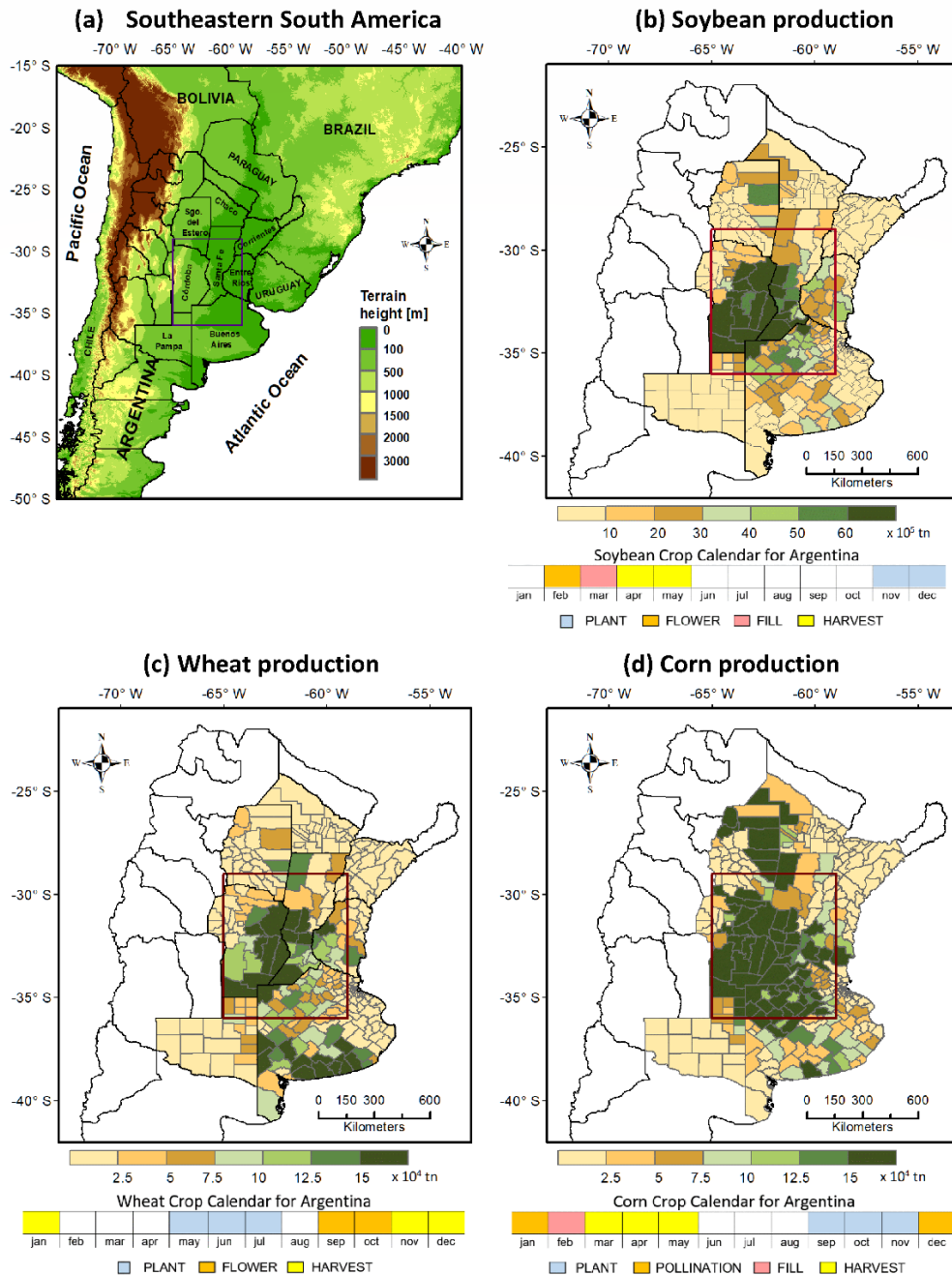
Figure 1: **(a)** Map of southern South America with topographic levels and country names. Relevant Argentina's provinces are identified as well. Argentina's Core Crop Region (highlighted with a dark brown rectangle) is the most productive region for corn, wheat, and soybean. The magnitude of production in [tn] was taken from the seasons 2010/11-20017/18 for soybeans and corn and from 2010/11-2018/19 for wheat. The production magnitudes for soybean, wheat, and corn are presented in panels b,c, and d, respectively. The crops' development cycle is identified in the lower part of each panel. The periods of grain-filling and flowering represent the most growth-sensitive months. They are (Oct-Nov) for wheat, (Dec-Jan) for corn, and (Jan-Feb) for soybean (MAGPyA).
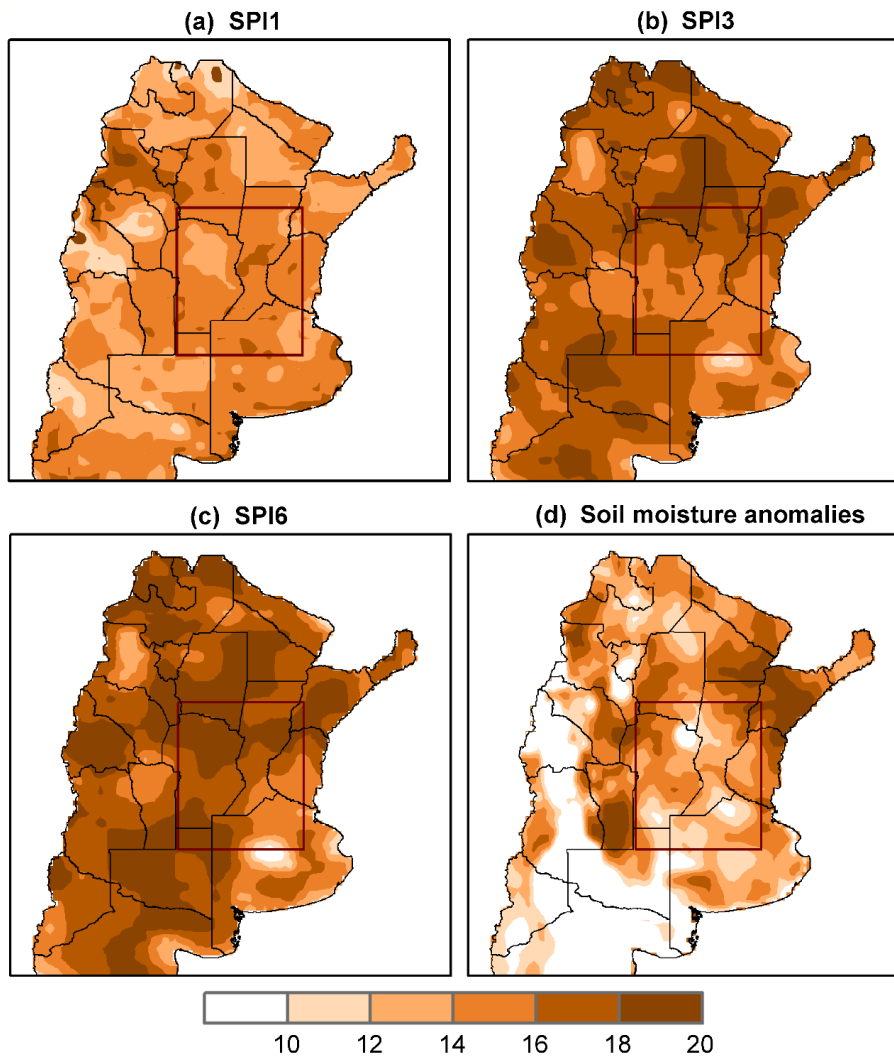
Figure 2: Percentage of months under moderate to extreme drought conditions (months below one standard deviation) of the total months from January 1979 to December 2018, according to (a) SPI1, (b) SPI3, (c) SPI6, and (d) soil moisture anomalies.

620
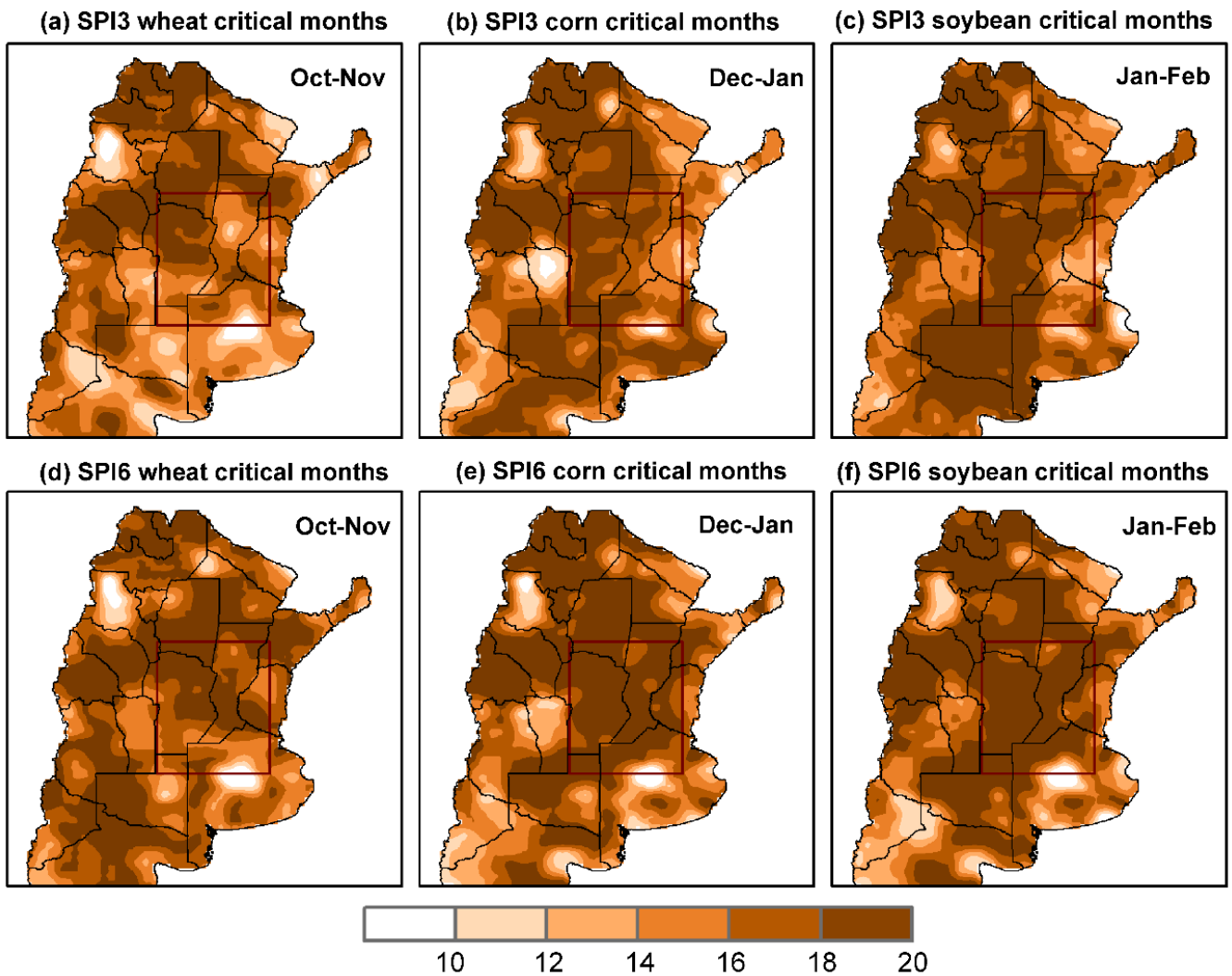
Figure 3: Percentage of months under moderate to extreme drought conditions (months below one standard deviation) during the crops' critical growing months from January 1979 to December 2018. For SPI3: (a) wheat during (Oct-Nov), (b) corn during (Dec-Jan), (c) soybean during (Jan-Feb). Panels (d), (e), and (f) are the same but for SPI6.
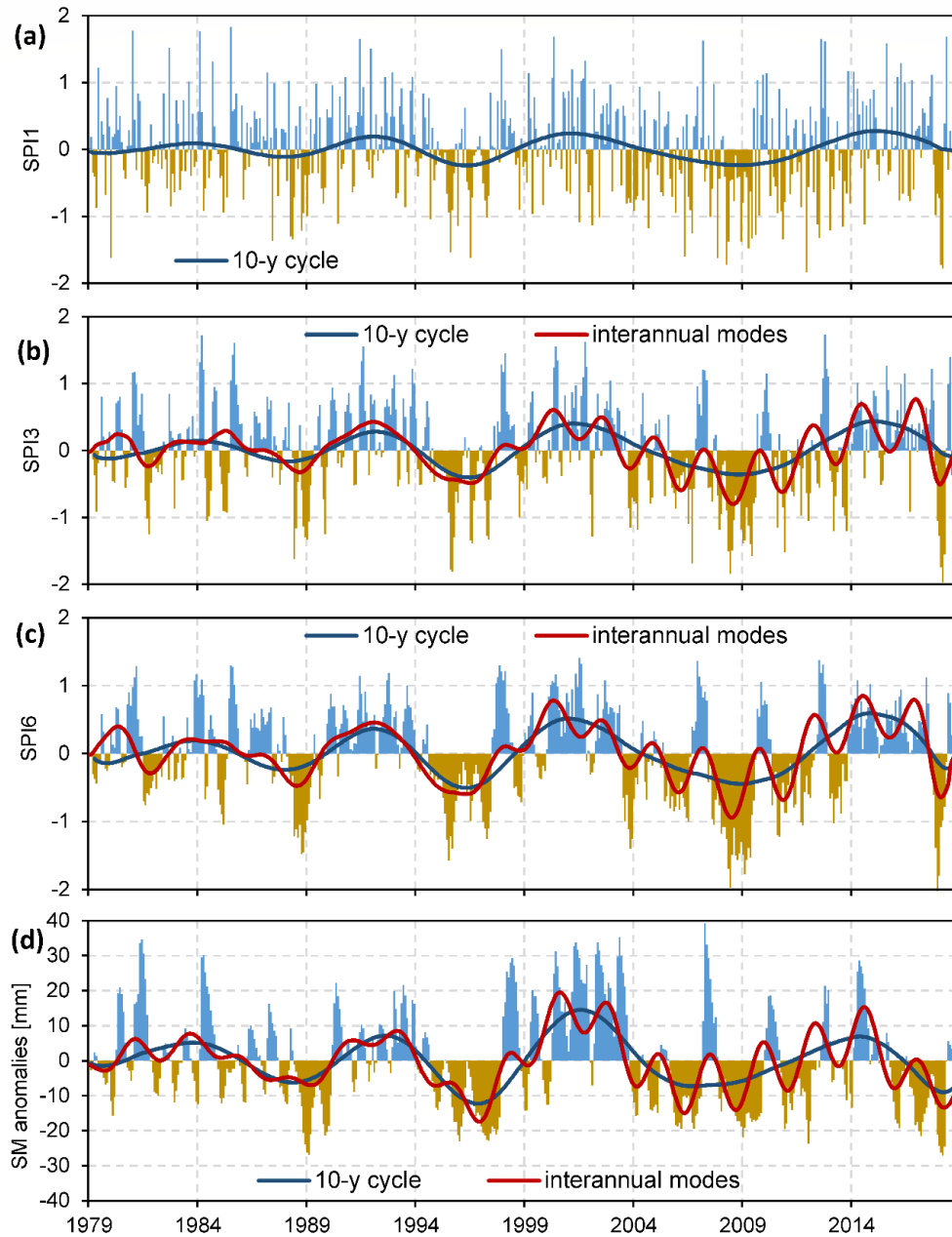
Figure 4: Areal-averaged time series from January 1979 to December 2018 for (a) SPI1, (b) SPI3, (c) SPI6, and (d) soil moisture anomalies in the Core Crop Region. The dominant modes of interannual variability are plotted in full lines.
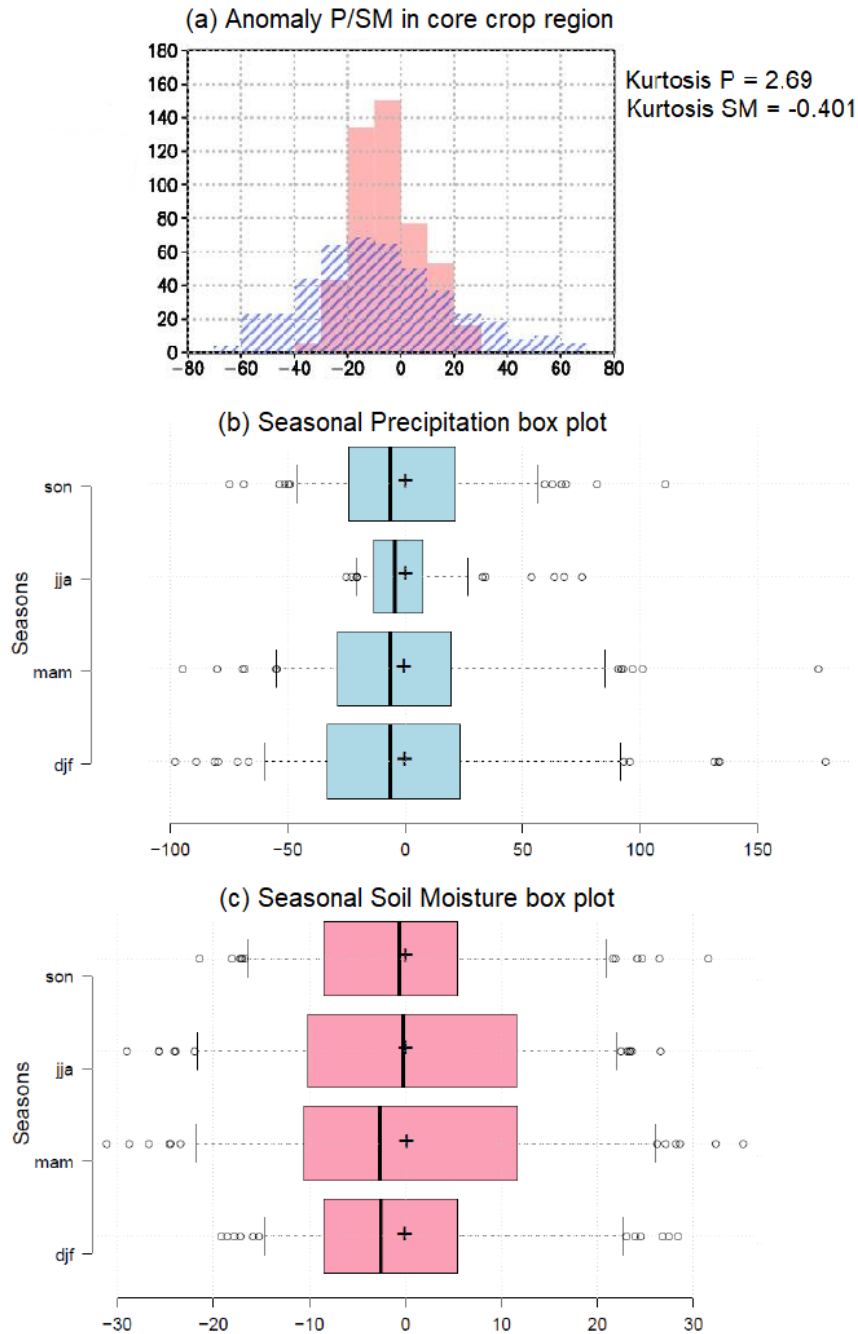
630

Figure 5: Frequency histograms in Core Crop Region and Kurtosis values for (a) Precipitation anomalies (blue-hatched) and soil moisture anomalies (light red); (b) boxplots of seasonally averaged time-series inside Core Crop Region for precipitation anomalies; (c) same as (b) but for soil moisture anomalies (light red). All computations were done from January 1979 to December 2018.

635
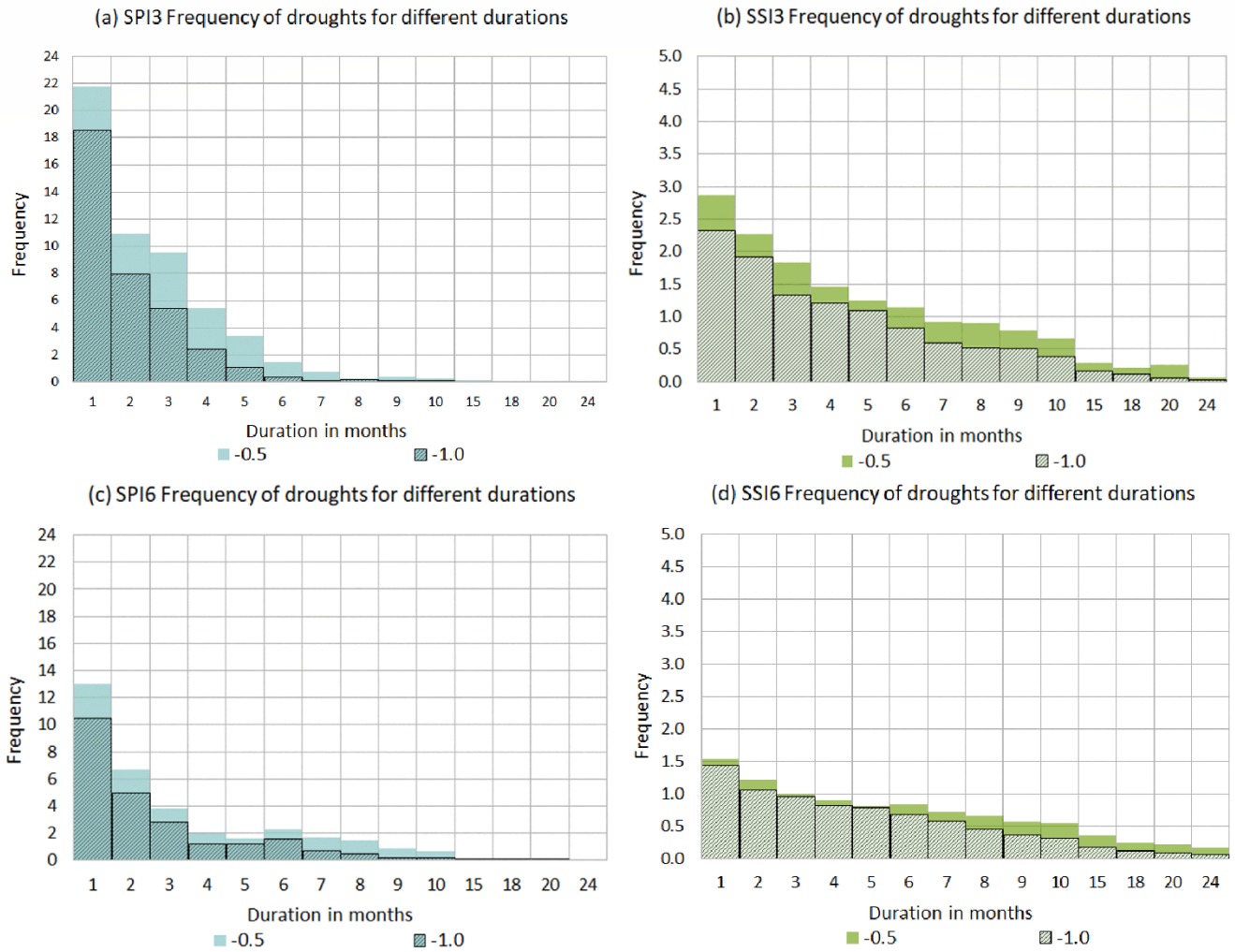
Figure 6: Histograms of droughts for different durations (in months) in the Core Crop Region. (a) SPI3, (b) SSI3, (c) SPI6, and (d) SSI6. Color bars indicate mild to extreme droughts whose values are less than $X_1 = -0.5$. Hatched bars in all the panels indicate moderate to extreme droughts whose values are less than $X_2 = -1$. All computations were done from January 1979 to December 2018.

640

645
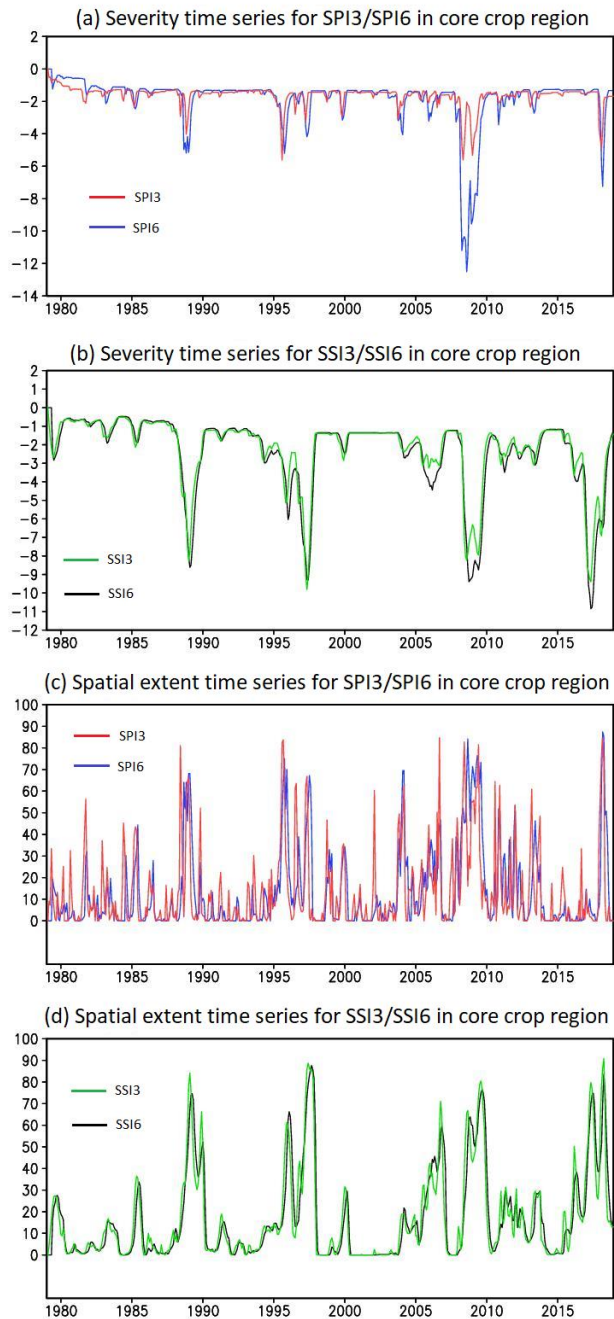
Figure 7: (a) Average time-series of drought severity for events below X_2 in the Core Crop Region based on SPI3 and SPI6 Indices; (b) as panel (a), but for SSI3 and SSI6; (c) Average time-series of the droughts' spatial extent for events below X_2 as a percentage of the Core Crop region's total area based on SPI3 and SPI6 indices; (d) as panel (c) but for SSI3 and SSI6. All computations were done from January 1979 to December 2018.

655
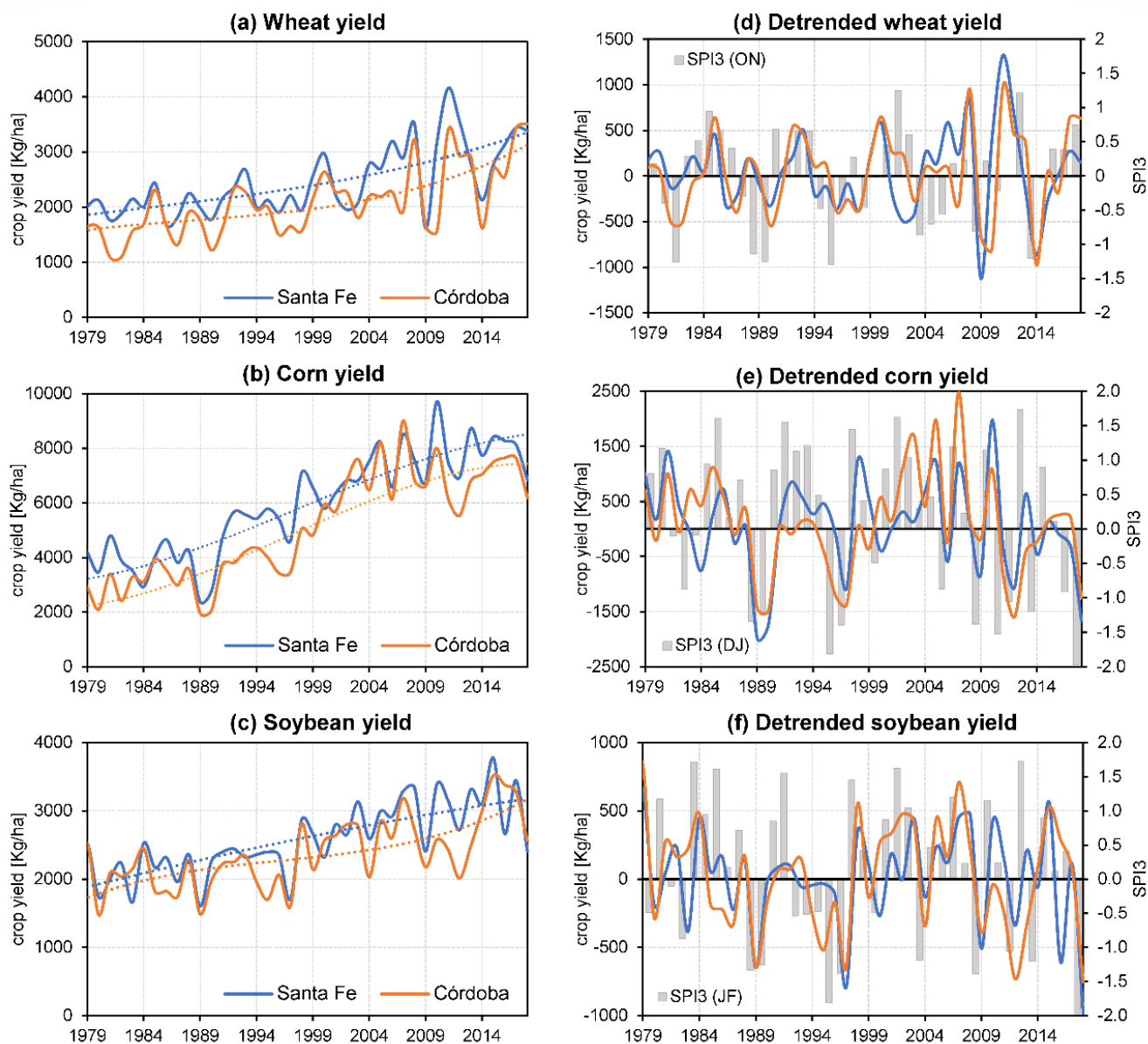
Figure 8: The time series of the area-averaged annual crop yield over the provinces of Santa Fe and Córdoba from 1979 to 2018. (a) Wheat; (b) Corn; (c) Soybean. Cubic polynomial trends are shown in dotted lines. Panels d-f present the detrended yields for Santa Fe (blue) and Cordoba (orange). The superimposed gray bars characterize the SPI3 values corresponding to the crops' critical growing months: ON for wheat, DJ for corn, and JF for soybean.